

Liftoff of a 60mg flapping-wing MAV

R.J. Wood

School of Engineering & Applied Sciences

Harvard University

Cambridge, MA 02138

rjwood@eecs.harvard.edu

Abstract—Up to this point, researchers working to artificially re-create hovering insect flight have not demonstrated an integrated micromechanical device that is able to lift its own weight. Inspiration from biological systems coupled with revolutionary breakthroughs in microfabrication technologies have now enabled the realization of insect-sized micro air vehicles (MAVs). This work describes a solution to the mechanical and aeromechanical components of an insect-scale MAV by demonstrating a 60mg structure that can generate sufficient lift to takeoff with external power and constrained body degrees of freedom.

I. INTRODUCTION

There have been various approaches taken in the pursuit of creating a mechanical solution for centimeter-scale MAVs. As an introduction to the MAV that is described here, it is appropriate to first give an overview of similar research on flapping wing MAVs and other centimeter-scale MAVs. These will be generally split into two categories: flapping-wing and rotary-wing.

Researchers at U.C. Berkeley have made tremendous progress in generating biologically-inspired wing trajectories using parallel mechanisms and piezoelectric actuators [1], [2], [3]. Piezoelectric actuators were also used as part of a tuned resonant drive for another two-wing MAV by a group at Vanderbilt [4], [5]. Researchers at the University of Tokyo have mimicked butterfly flight with a 400mg, 14cm wingspan MAV [6]. An alternate approach uses reciprocating chemical muscles to power a 50 gram flapping wing device called the ‘Entomopter’ [7]. On a similar scale, researchers from Caltech and Aerovironment created an RC flapping-wing MAV based upon mammalian flight called the ‘Microbat’ [8], [9], [10]. This ornithopter was able to demonstrate sustained controlled flight for greater than six minutes. Similarly, a group at the University of Delaware has constructed a small ornithopter using rotary and parallel mechanisms [11], [12].

In addition to flapping-wing versions, there have also been a number of attempts to create centimeter-scale rotary-wing MAVs. One of the most ambitious was the ‘Mesocopter’ at Stanford [13], [14]. This was a quad-rotor, 1.5cm, battery powered system that was able to demonstrate thrust. There have been other successful

demonstrations of rotary-wing MAVs from developers in industry (e.g. Seiko-Epson 12.3g μ FR-II [15]) and from private hobbyists (e.g. the 6.9g RC ‘Pixelito’ [16]).

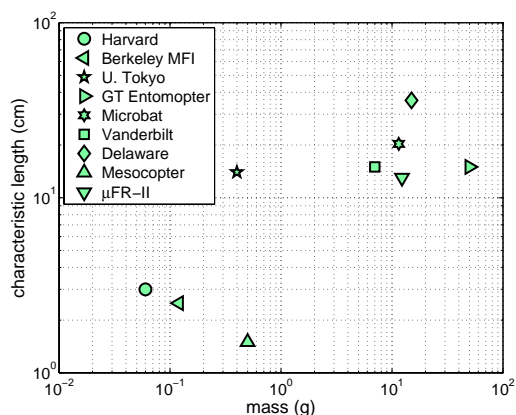


Fig. 1. Illustration of the length and mass properties of a number of MAVs. Fixed wing MAVs are not considered here.

This space of flapping-wing and rotary-wing MAVs is illustrated in Fig. 1. All of these examples have similar underlying goals:

- 1) **maneuverability:** A metric to describe the maneuverability of an air vehicle is the inverse of the turning radius. In this sense, hovering is ideal and allows the MAV to operate in constricted environments.
- 2) **small size:** Whether for stealth, portability, or multiplicity, centimeter-scale systems vastly expand the applications of more traditional UAVs.
- 3) **propulsive efficiency:** Peak thrust and mission duration are directly related to the aeromechanical propulsive efficiency. Traditional lift mechanisms typically lose efficiency as size decreases. However, small MAVs can potentially take advantage of a number of unique aerodynamic phenomena.

A MAV with similar size and flight principles as Dipteran insects could address each of these points in a way that would exceed most of the examples from current and past research. This paper describes

the fabrication and results from a 60mg, 3cm wingspan biologically-inspired MAV that is the first insect-sized device to demonstrate sufficient lift to takeoff vertically. This microrobot is shown in Fig. 2.

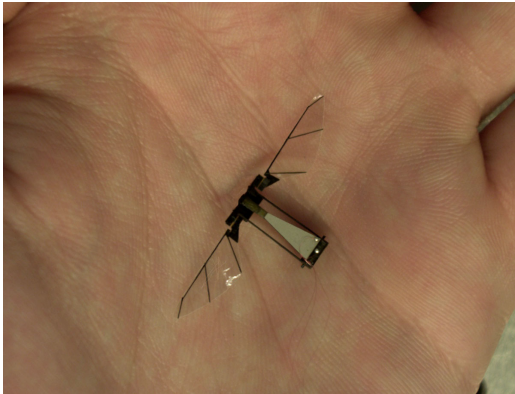


Fig. 2. Completed 60mg, 3cm wingspan MAV.

II. FABRICATION

Each component (mechanical, mechatronic, aeromechanical) is constructed using a new microfabrication paradigm called Smart Composite Microstructures (SCM) [17]. This entails laminated, laser micromachined components arranged to create rigid links, compliant flexure joints, and actuators. The major components of SCM are shown in Fig. 3. All components of the fly are created with this process and moreover these results act as a validation of the merits of SCM.

A. Actuator

Small size limits the choice of actuation technology. Further, there are baseline metrics that need to be met to make flight feasible: most important are power density and efficiency. Biological estimates put the body-mass-specific power density for flying insects at 29W/kg [18] and 40W/kg [19] and 80W/kg [20] and 83W/kg [21] for

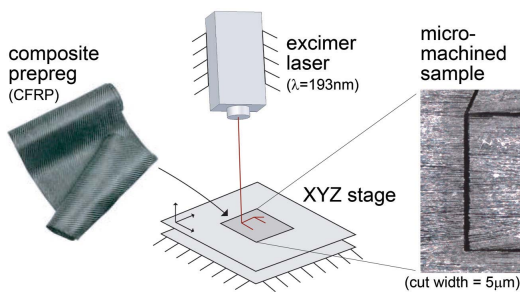


Fig. 3. Overview of the smart composite microstructures process. First, thin laminae (typically composite materials and polymers) are laser-micromachined, stacked, and cured together. Once released, flexures are formed as gaps between rigid links. If electroactive materials are included in the laminate, actuators are created.

the muscles alone. There is no evidence that biological muscles are optimal, but these numbers are useful as minimum values that need to be achieved by MAV actuators. Several candidate technologies are presented in tab. I.

From these options, bulk piezoelectric materials are chosen for high bandwidth, power density, and efficiency, and also for the ease of including such materials into the SCM process. Bimorph bending cantilever actuators are created from amorphous PZT-5H plates and passive composite materials. The models for these actuators are now sufficiently mature to be used as design tools to predict the static and dynamic properties of the actuator [25], [26]. A completed 40mg, 13mm actuator is shown in Fig. 4. Similar actuators made with the same process have demonstrated power densities as high as 400W/kg [27].

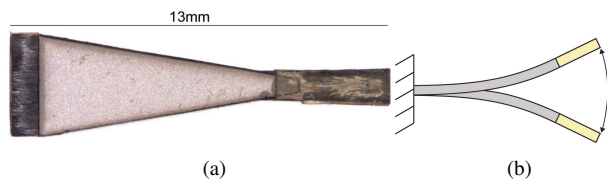


Fig. 4. Piezoelectric bending cantilever microactuator (a) and (exaggerated) motion (b).

B. Thorax

An intermediate linkage between the actuator input and the wing motion is a transmission mechanism called the ‘thorax’ [28]. This consists of a mechanical amplification system created with low-loss compliant joints to impedance match the actuator to the wing loading. This is also very similar to an insect thorax in the sense that relatively small actuator motion is used to resonate a compliant structure to produce a large wing stroke. In this case, there is only one actuated degree-of-freedom (DOF) which is the stroke angle. Flexures in the wing-hinge allow the wing to passively rotate along an axis parallel to the span-wise direction and joint-stops incorporated into these flexures eliminate over rotation. This structure is shown in Fig. 5.

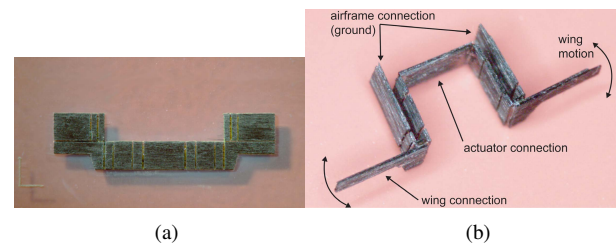


Fig. 5. Transmission system post-cure (a) and completed (b).

TABLE I
QUALITATIVE COMPARISON OF ACTUATION TECHNOLOGIES.

●=highest, ◐=high, ◑=moderate, ◒=low, ○=lowest

| type | example | efficiency | toughness | bandwidth ¹ | max. ϵ | max. σ | density |
|----------------|------------------------|------------|-----------|------------------------|-----------------|---------------|---------|
| bulk piezo. | PZT-5H ² | ◑ | ◑ | ● | ○ | ◐ | ● |
| single crystal | PZN-PT ³ | ◑ | ○ | ● | ◐ | ◐ | ● |
| AFC | PZT-5A ⁴ | ◑ | ◐ | ● | ◐ | ◐ | ◐ |
| SMA | Nitinol ⁵ | ○ | ◐ | ◐ | ◐ | ● | ● |
| IPMC | Nafion ⁶ | ◑ | ◐ | ◐ | ● | ◐ | ◐ |
| EAP | DE ⁷ | ◑ | ◐ | ◐ | ● | ◐ | ◐ |
| electromag. | brushless ⁸ | ◐ | NA | ◐ | NA | NA | ● |

¹depends upon structure geometry

²from Piezo Systems, <http://www.piezo.com>

³single crystal piezoelectric ceramics, see [22]

⁴active fiber composites from Advanced Cerametrics, <http://www.advancedcerametrics.com>

⁵shape memory alloy, <http://www.dynalloy.com>

⁶from DuPont, see [23]

⁷dielectric elastomers, see [24]

⁸for example 0308 brushless DC micro-motor from Smoovy, <http://www.faulhaber-group.com>

C. Airframe

The airframe is very minimal and has a simple design goal: provide a solid mechanical ground to the actuator base and transmission. To achieve this, a rectangular truss is created as is shown in Fig. 6. This airframe is constructed entirely from ultra-high modulus carbon fiber composite materials to create an extremely rigid, lightweight mechanical ground.

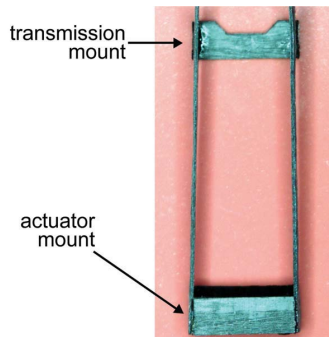


Fig. 6. Completed airframe.

D. Wings

The airfoils are created as a combination of rigid ‘veins’ and a thin film ‘membrane’. This is directly analogous to the reinforcement structure of most insect wings [29], [30], but instead of chitin, carbon fiber is used. The veins are laser-micromachined and aligned to a predetermined pattern and cured to a $1.5\mu\text{m}$ polymer face sheet. The resulting airfoils are shown in Fig. 7. At approximately 400 micrograms and 15mm long, these

wings see a loading of approximately 1Nm^{-2} and have the highest strength-to-weight ratio of any airfoil (man-made or biological) ever created.

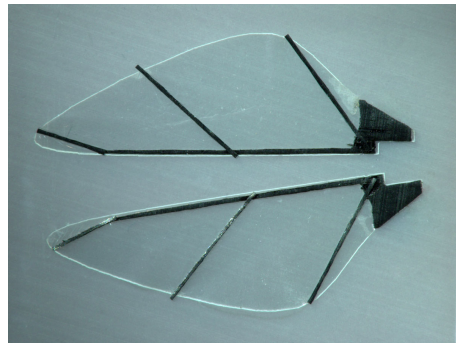


Fig. 7. Completed airfoils.

E. Integration

Following the completion of the four principle elements, the wings, thorax, and actuator are integrated onto the airframe. Since all crucial alignment is done with the laser micromachining system as part of the SCM process, there is little chance of error in the final assembly. As a highlight of the virtue of SCM, all components can be created and integrated onto a complete microrobotic fly in less than one week. The final mass properties for each element are given in tab. II.

TABLE II
MASS PROPERTIES FOR EACH COMPONENT OF THE MAV.

| component | mass (mg) |
|-------------------------------|---------------|
| actuator | 40 |
| transmission | 4 |
| wings ($\times 2$) | ≈ 0.5 |
| airframe | 11 |
| total body¹ | 60 |

¹there is unaccounted for mass from wiring, epoxy, etc.

III. ANALYSIS

There are two focuses of the analysis: the wing trajectory that the robotic fly can achieve and the ability to generate lift sufficient for sustained flight.

A. Benchtop

The wing trajectory was evaluated with a benchtop structure. Here the fly was rigidly fixed to ground and the wings are driven open-loop at the flapping resonance to attain as large an angular wing stroke as possible. It should be noted that the design of the passive wing hinge is crucial such that the rotational resonant mode is sufficiently higher than the flapping resonance (so that the rotation is quasi-static). The experimental flapping resonance is 110Hz and the predicted rotational resonance is approximately 250Hz. The visualization from a high-speed video camera (shown in Fig. 8) is quite remarkable. The wings exhibit a trajectory nearly identical to biological counterparts. At the start of each half-stroke, an attached vortex is formed at the leading edge. This vortex grows in strength until an equilibrium magnitude is reached and the vortex is stabilized. If wing reversal happens too quickly, this vorticity does not have time to reach full strength and the average lift will be diminished. With a wing length of 15mm, average chord length of 3mm, and maximum swept angle of approximately 110° , the wing moves approximately 10 chord lengths at each half-stroke. This wing stroke should be an ample distance to allow the leading-edge vortex to stabilize [31]. Lift measurements show a thrust-to-weight ratio of ≈ 2 [28].

B. Liftoff

After integration, the fly is fixed to guide wires that restrict the motion such that the fly can only move in the vertical direction. These guides represent a set of ‘training wheels’ that will be iteratively removed in future generations once attitude control is realized. There are slots in the back of the airframe that give the fly proper alignment to the guide wires. If the guides are spaced properly, there is no friction acting between the fly and the wires and the wires act only to eliminate roll, pitch, and yaw. Electrical connection is made using three $25\mu\text{m}$ diameter wires to avoid any

elasticity and minimize the added mass. Specifications for the completed fly are given in tab. III. The wings are again driven open-loop at resonance (ramping the amplitude up from zero) and the fly rapidly ascends as is shown in Fig. 9.

TABLE III
INTEGRATED MAV PERFORMANCE.

| | |
|----------------------------|------------------------|
| total mass | 60mg |
| wingspan | 3cm |
| actuator power dens. | $> 150\text{Wkg}^{-1}$ |
| total power dens. | $> 100\text{Wkg}^{-1}$ |
| wing stroke | $> \pm 50^\circ$ |
| wing rotation | $\pm 50^\circ$ |
| wingbeat frequency | 110Hz |
| wing velocity ¹ | $> 6\text{ms}^{-1}$ |
| Reynolds num. ¹ | ≈ 1200 |

¹maximum

IV. DISCUSSION

These results only present one possible aeromechanical solution for the creation of an insect-sized MAV, however this is a significant step towards the realization of autonomous flying microrobots. This also opens numerous doors for exploration including initial control experiments, optimization of thrust, incorporation of additional controlled DOFs to begin attitude control, additional wings, etc. However, it also highlights the importance of other research paths such as the development of miniature power sources and creation of appropriate sensors and microelectronics to control flight.

ACKNOWLEDGEMENTS

Thanks to the Dickinson lab at Caltech, and the Fearing lab at U.C. Berkeley for helpful discussions.

REFERENCES

- [1] J. Yan, R. Wood, S. Avadhanula, and M. S. and R.S. Fearing, “Towards flapping wing control for a micromechanical flying insect,” in *IEEE Int. Conf. on Robotics and Automation*, Seoul, Korea, May 2001.
- [2] S. Avadhanula, R. Wood, E. Steltz, J. Yan, and R. Fearing, “Lift force improvements for the micromechanical flying insect,” in *IEEE/RSJ Int. Conf. on Intelligent Robots and Systems*, Las Vegas, Nevada, Oct. 2003.
- [3] S. Avadhanula, R. Wood, D. Campolo, and R. Fearing, “Dynamically tuned design of the MFI thorax,” in *IEEE Int. Conf. on Robotics and Automation*, Washington, DC, May 2002.
- [4] A. Cox, D. Monopoli, M. Goldfarb, and E. Garcia, “The development of piezoelectrically actuated micro-air vehicles,” in *SPIE Conf. on Microrobotics and Microassembly*, vol. 3834, Boston, Massachusetts, Sept. 1999, pp. 101–108.
- [5] A. Cox, D. Monopoli, D. Cveticanin, M. Goldfarb, and E. Garcia, “The development of elastodynamic components for piezoelectrically actuated flapping micro-air vehicles,” in *J. of Intelligent Material Systems and Structures*, vol. 13, Sept. 2002, pp. 611–615.
- [6] H. Tanaka, K. Hoshino, K. Matsumoto, and I. Shimoyama, “Flight dynamics of a butterfly-type ornithopter,” in *IEEE/RSJ Int. Conf. on Intelligent Robots and Systems*, Edmonton, Alberta, Canada, 2005.

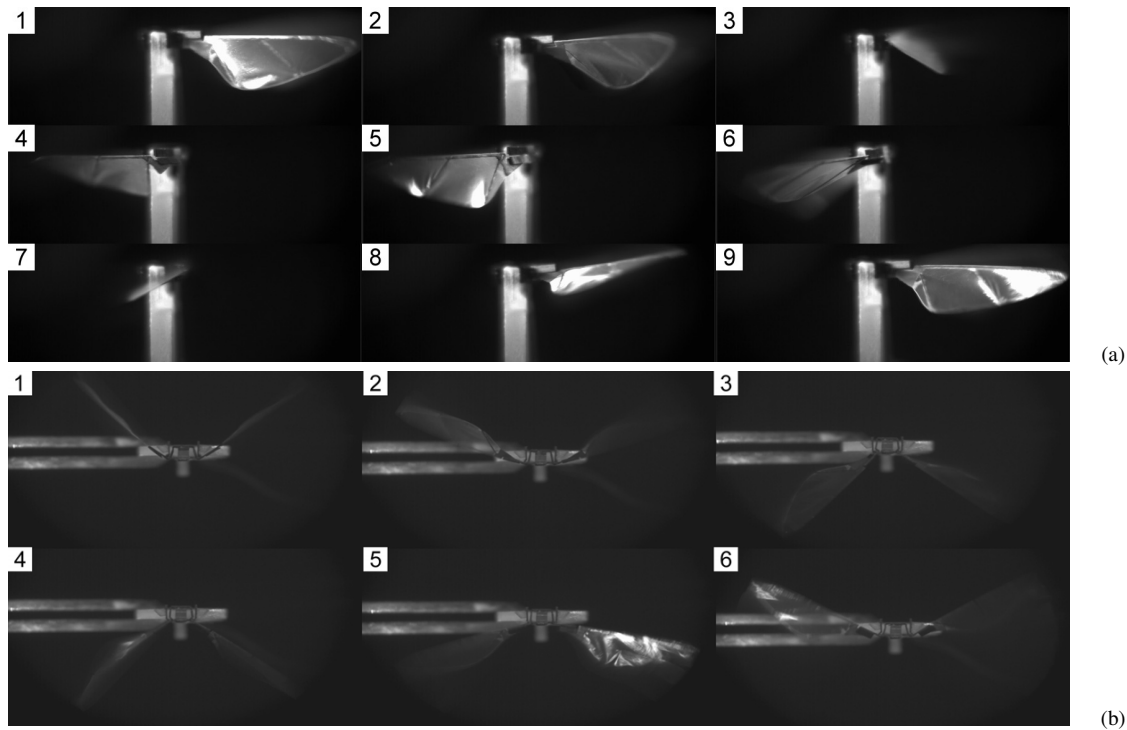


Fig. 8. Wing motion as seen from a side perspective (a) and an anterior perspective (b). These are frames from a high speed video sequence of the wing moving at its flapping resonance. The side perspective is taken at mid-stroke: note the symmetry and that the angle of attack at mid-stroke is approximately 50° .

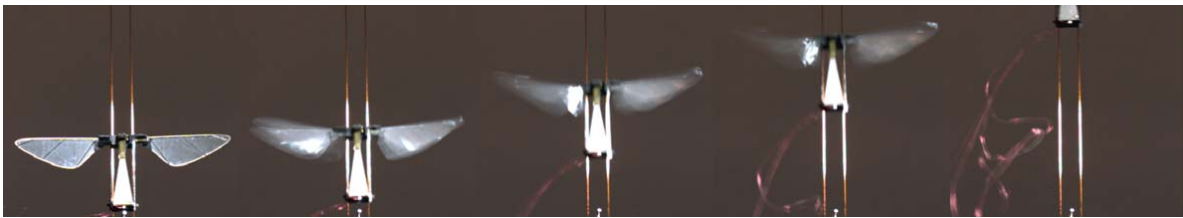


Fig. 9. The first tethered flight of an at-scale robotic insect.

- [7] R. Michelson, "The entomopter," in *Neurotechnology for Biomimetic Robots*. The MIT Press, Sept. 2002, pp. 481–509.
- [8] T. Pornsin-Shiriak, Y. Tai, H. Nassef, and C. Ho, "Titanium-alloy MEMS wing technology for a micro aerial vehicle application," *J. of Sensors and Actuators A: Physical*, vol. 89, pp. 95–103, Mar. 2001.
- [9] T. Pornsin, S. Lee, H. Nassef, J. Grasmeyer, Y. Tai, C. Ho, and M. Keennon, "Mems wing technology for a battery powered ornithopter," in *The 13th IEEE Annual Intl. Conf. on MEMS*, Miyazaki, Japan, Jan. 2000, pp. 709–804.
- [10] M. Keennon and J. Grasmeyer, "Development of the Black Widow and Microbat MAVs and a vision of the future of MAV design," in *AIAA/ICAS Intl. Air and Space Symp. and Exposition: The Next 100 Years*, Dayton, OH, July 2003.
- [11] R. Madangopal, Z. Khan, and S. Agrawal, "Biologically inspired design of small flapping wing air vehicles using four-bar mechanisms and quasi-steady aerodynamics," *J. of Mech. Design*, vol. 127, pp. 809–816, July 2005.
- [12] Z. Khan and S. Agrawal, "Design of flapping mechanisms based on transverse bending phenomena in insects," in *IEEE Int. Conf. on Robotics and Automation*, Orlando, FL, May 2006, pp. 2323–2328.
- [13] I. Kroo and P. Kunz, "Development of the mesicopter: A miniature autonomous rotorcraft," in *American Helicopter Society International Vertical Lift Aircraft Design Specialists Meeting*, San Francisco, CA, Jan. 2000.
- [14] —, "Meso-scale flight and miniature rotorcraft development," in *Fixed and Flapping Wing Aerodynamics for Micro Air Vehicle Applications*, ser. Progress in Astronautics and Aeronautics, vol. 195. American Institute of Aeronautics and Astronautics, 2001.
- [15] http://www.epson.co.jp/e/newsroom/news_2004_08_18.htm.
- [16] <http://pixelito.reference.be/>.
- [17] R. Wood, S. Avadhanula, R. Sahai, E. Steltz, and R. Fearing, "Microrobot design using fiber reinforced composites," *to appear: J. of Mechanical Design*, 2007.
- [18] M. Sun and J. Wu, "Aerodynamic force generation and power requirements in forward flight in a fruit fly with modeled wing motion," *J. of Experimental Biology*, vol. 206, pp. 3065–3083, 2003.
- [19] M. Dickinson and J. Lighton, "Muscle efficiency and elastic storage in the flight motor of *Drosophila*," *Science*, vol. 268, pp. 87–90, Apr. 1995.
- [20] F.-O. Lehmann and M. Dickinson, "The changes in power requirements and muscle efficiency during elevated force production in the fruit fly *Drosophila Melanogaster*," *J. of Experimental Biology*, vol. 200, pp. 1133–1143, 1997.

- [21] M. Tu and T. Daniel, "Submaximal power output from the dorsolongitudinal flight muscles of the hawkmoth *Manduca sexta*," *J. of Experimental Biology*, vol. 207, pp. 4561–4662, 2004.
- [22] J. Yin, B. Jiang, and W. Cao, "Elastic, piezoelectric, and dielectric properties of $0.995\text{Pb}(\text{Zn}_{1/3}\text{Nb}_{2/3})\text{O}_3 - 0.45\text{PbTiO}_3$ single crystal with designed multidomains," *IEEE Trans. on Ultrasonics, Ferroelectrics, and Frequency Control*, vol. 47, no. 1, pp. 285–291, Jan. 2000.
- [23] S. Lee, H. Park, and K. Kim, "Equivalent modeling for ionic polymermetal composite actuators based on beam theories," *Smart Materials and Structures*, vol. 14, no. 6, pp. 1363–1368, Dec. 2005.
- [24] R. Pelrine, P. Sommer-Larsen, R. Kornbluh, R. Heydt, G. Kofod, Q. Pei, and P. Gravesen, "Applications of dielectric elastomer actuators," in *Proc. of Int. Soc. Opt. Eng.*, vol. 4329, 2001, pp. 335–349.
- [25] R. Wood, E. Steltz, and R. Fearing, "Optimal energy density piezoelectric bending actuators," *J. of Sensors and Actuators A: Physical*, vol. 119, no. 2, pp. 476–488, 2005.
- [26] —, "Nonlinear performance limits for high energy density piezoelectric bending actuators," in *IEEE Int. Conf. on Robotics and Automation*, Barcelona, Spain, Apr. 2005.
- [27] E. Steltz and R. Fearing, "Dynamometer power output measurements of piezoelectric actuators," in *IEEE/RSJ Int. Conf. on Intelligent Robots and Systems*, San Diego, CA, Oct. 2007.
- [28] R. Wood, "Design, fabrication, and analysis, of a 3DOF, 3cm flapping-wing MAV," in *IEEE/RSJ Int. Conf. on Intelligent Robots and Systems*, San Diego, CA, Oct. 2007.
- [29] S. Combes and T. Daniel, "Flexural stiffness in insect wings I. Scaling and the influence of wing venation," *J. of Experimental Biology*, vol. 206, pp. 2979–2987, 2003.
- [30] —, "Flexural stiffness in insect wings II. Spacial distribution and dynamic wing bending," *J. of Experimental Biology*, vol. 206, pp. 2989–2997, 2003.
- [31] R. Dudley, *The Biomechanics of Insect Flight: Form, Function and Evolution*. Princeton University Press, 1999.